

Materiales



## MAGNETIC HEATING ABILITY OF SILICA-COBALT FERRITE NANOPARTICLES

### CAPACIDAD DE CALENTAMIENTO MAGNÉTICO DE NANOPARTÍCULAS DE SÍLICA-FERRITA DE COBALTO

M.E. Cano<sup>2</sup>, R.H. Medina<sup>1</sup>, V.V.A. Fernández<sup>2</sup> and P.E. García-Casillas<sup>1\*</sup>

<sup>1</sup>Instituto de Ingeniería y Tecnología de Universidad Autónoma de Ciudad Juárez, Av. del Charo 620 Nte., Col. Partido Romero, Ciudad Juárez, Chihuahua, México.

<sup>2</sup>Centro Universitario de la Ciénega de la Universidad de Guadalajara, Av. Universidad 1115, col. Linda Vista, Ocotlán, Jalisco, México.

Received April 1 2013; Accepted February 6 2014

#### Abstract

In this study, the magnetic induction heating of cobalt ferrite nanoparticles with or without silica coating was analyzed for evaluating the feasibility of these materials to be used for magnetic hyperthermia. Particles of approximately 14 and 40 nm were evaluated. For this purpose, we used a magnetic induction system to obtain the specific absorption rate (SAR) values. Two different amplitudes of 35 mT and 63 mT at 180 kHz were used. Our results showed the smaller particles exhibiting the higher SAR value, independent of the intensities applied. Moreover, there was no significant change in the SAR values for both particle sizes in presence of silica. However, silica increased the hydrolytic degradation.

**Keywords:** cobalt ferrite, hyperthermia, magnetic induction, nanomaterials, ferromagnetism.

#### Resumen

En este estudio, el calentamiento por inducción magnética de nanopartículas de ferrita de cobalto con o sin recubrimiento de sílice fueron analizados para evaluar la viabilidad de estos materiales para ser utilizados en tratamiento de hipertermia magnética. Las partículas evaluadas tienen un tamaño entre 14 y 40 nm aproximadamente. Para este propósito, se utilizó un sistema de inducción magnética obteniendo la tasa de absorción específica valores (SAR, por sus siglas en inglés). Se utilizaron dos diferentes amplitudes de 35 mT y 63 mT a 180 kHz. Estos resultados muestran que las partículas más pequeñas presentan el valor más alto de SAR, independiente de las intensidades aplicadas. Por otra parte, no hubo ningún cambio significativo en los valores de SAR para ambos tamaños de partículas cuando estas partículas contienen sílice. Sin embargo, sílice aumentó la degradación hidrolítica.

**Palabras clave:** ferrita de cobalto, hipertermia, inducción magnética, nanomateriales, ferromagnetismo.

## 1 Introduction

Magnetic nanoparticles are at the forefront of the most promising materials for clinical diagnostic and therapeutic applications. They are widely used for labeling and manipulating biomolecules, targeting drugs and genes, magnetic resonance imaging, and hyperthermia treatment (Varadan *et al.*, 2008; Cornell

*et al.*, 2003). The iron oxides nanoparticles are the most utilized magnetic material for biomedical applications because of their magnetic behavior. Moreover, functionalized surfaces of such materials can bond with different molecules, allowing the manipulation with an external field (Cullity *et*

\*Autora para la correspondencia. E-mail: pegarcia@uacj.mx  
Tel. (656) 6884887

*al.*, 2009; Neuberger *et al.*, 2005). However, the current researches in this field are mainly targeted to develop multifunctional systems suitable for performing two or more therapeutics actions simultaneously, for instance, drug delivery and magnetic hyperthermia. Due to the similarity in crystal structure to magnetite, cobalt ferrite is an interesting material in this regard. This compound also transmits heat in presence of an external alternating magnetic field. In order to transform the cobalt ferrite in a multifunctional material, its surface must be modified with biocompatible and biodegradable materials which improve their chemical stability as well as ensure the ability to bind with biological entities. The objective of our current research was to modify the cobalt-ferrite surfaces in such a way that makes the material suitable for therapeutic usages. Here we present the synthesis of cobalt ferrite nanoparticles coated with silica and the results related to their heating ability and degradation rate in a body-simulated fluid in presence of an external field.

## 2 Experimental procedure

### 2.1 Cobalt ferrite synthesis

For the synthesis of cobalt ferrite ( $\text{CoFe}_2\text{O}_4$ ), 6.91 g of  $\text{FeCl}_3 \cdot 6\text{H}_2\text{O}$  and 3.72 g of  $\text{Co}(\text{NO}_3)_2 \cdot 7\text{H}_2\text{O}$  were first dissolved in 20 ml of distilled water. Ammonium hydroxide was then added into the solution in order to increase the pH value to 11. The black precipitate formed at about 80 °C was washed several times using magnetic separation method until the supernatant reached a pH value of 7. The powder was then dried at  $30^\circ \pm 5^\circ \text{C}$  for 24 h and finally calcined either at 500° or 700 °C to obtain the crystalline structure.

### 2.2 Synthesis of silica-coated nanoparticles

Silica-coated cobalt ferrite nanoparticles ( $\text{CoFe}_2\text{O}_4/\text{SiO}_2$ ) were synthesized by hydrolysis of sodium methasilicate ( $\text{Na}_2\text{SiO}_3$ ). For this purpose, 2 g of  $\text{Na}_2\text{SiO}_3$  was dissolved in 20 ml of distilled water by sonication. The required quantity of cobalt ferrite nanoparticles was subsequently added into the solution, keeping a  $\text{NaSiO}_3/\text{CoFe}_2\text{O}_4$  weight ratio of 10:1. The resulting solution was sonicated for 45 minutes to initiate the interaction between these two compounds. Subsequently, the temperature of the solution was increased to 80 °C, and hydrochloric acid (12.5 %) was added drop-wise at 80 °C until the solution reached a pH of 9. The precipitate was washed

several times with distilled water until it reached a pH of 7. The solid was finally dried.

### 2.3 Induction heating

The induction heating ability of particles was evaluated from the temperature vs. time curves. A small portion of particles (see table I), suspended and dispersed in 0.5 ml of water, was placed in a magnetic induction device following the procedure reported elsewhere (Ming *et al.*, 2004; Cano *et al.*, 2012; Cano *et al.*, 2011). The sample was placed in cylindrical tube of 2 ml and 9 mm diameter. The magnetic field employed was 35 mT and 63 mT (through a coil of three turns, diameter 3 cm and 2 cm of length) and a constant frequency  $f = 180$  kHz. The temperature was measured using a fluoroptic thermometer (IPITEK 500) and a thin optical fiber transducer to avoid interactions with the magnetic field. We also monitored the indications of sample positioning, sensor location, diameter, and volume of samples to diminish the errors sources following the previous reports (Huang *et al.*, 2012; Wang *et al.*, 2013). We calculated the specific absorption rate (SAR) value using Equation 1 (Ruizhi *et al.*, 2007; Goya *et al.*, 2008).

$$SAR = C \frac{\Delta T}{\Delta t} \frac{1}{m} \quad (1)$$

Where  $\Delta T/\Delta t$  is the initial slope of the time-dependent temperature curve,  $m$  is the ratio of the mass suspension medium and the mass of nanoparticles, and  $C$  is the total specific heat of the sample. For each sample, the initial slope value was calculated in the range of 5 to 20 seconds assuming a linear fit of the data. In some articles, the heat capacity of water is used to obtain the SAR value, but we calculated the effective specific heat  $C_{eff}$  from Equation 2, using the specific heat of the composites ( $C_{NP}$ ) and that of water ( $C = 4.16$  J/gK). These values were directly measured using a differential scanning calorimeter (DSC), Perkin Elmer DSC 6. The procedure involves the curves overlapping of the tested sample against a standard reference (Indium). The details are reported elsewhere (O'Neili, 1966). Before obtaining the specific heat, the samples were heated from 30° to 300° C to erase a possible thermal history.

$$C_{eff} = \frac{m_{H_2O}(4.16) + m_{NP}(C_{NP})}{m_{H_2O} + m_{NP}} \quad (2)$$

## 2.4 Hydrolytic degradation of nanoparticles

A phosphate buffer solution (PBS) was prepared by dissolving 8 g of NaCl, 0.2 g of KCl, 1.44 g of  $\text{Na}_2\text{HPO}_4$ , and 0.24g of  $\text{KH}_2\text{PO}_4$  in 800 ml of distilled water. The pH of the solution was adjusted to 7.4, and the solution was then sterilized in an autoclave. Thereafter, 50 mg of nanoparticles were added to 0.5 ml of PBS and stored at 37 °C for 6 -18 h. Finally, the nanoparticles were separated and washed with distilled water. The powder was dried at 27 °C until complete evaporation of water, and the dried nanoparticles were weighed.

## 3 Results and discussion

X-ray diffraction pattern confirmed the formation of the cubic structure (Fig. 1). The powders obtained at 500° and 700 °C showed the characteristic peaks of the  $\text{CoFe}_2\text{O}_4$  phase at  $2\theta = 18.5, 30.2, 35.6, 37.2, 43.2, 53.6, 57.2, 62.7, 71.2,$  and  $74.2$  corresponding to the planes (111), (220), (311), (222), (400), (422), (511), (440), and (533); thus indicating the phase obtained was of pure  $\text{CoFe}_2\text{O}_4$ . The average crystallite sizes were calculated from the X-ray patterns using Scherrer's equation, assuming a uniform distribution of particles. This equation involves the line broadening measurements (FWHM) of the most intense peak. The values obtained were very close to 13.7 nm and 40 nm for 500° and 700 °C, respectively. This analysis and procedure were also used by various authors before (Sanhueza *et al.*, 2011; Veverka *et al.*, 2007; Yeong II *et al.*, 2003).

The particle size distribution was determined from SEM images, following the procedure described by Gaumet *et al.* (2008). The average particle sizes were  $19 \pm 4$  nm and  $44 \pm 12$  nm for the sample obtained at 500° and 700 °C, respectively (Figs. 2A and C). These values are in good agreement to those obtained using Scherrer's model. Furthermore, the histograms of particles size showed a narrow distribution (Figs. 2 B and D).

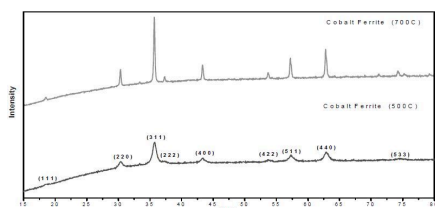


Fig. 1. X ray pattern of the  $\text{CoFe}_2\text{O}_4$  obtained at 500 and 700 °C.

The silica coating of the  $\text{CoFe}_2\text{O}_4$  nanoparticles was confirmed by FT-IR spectroscopy. Figure 3 shows the characteristic band of Si-O interaction at about  $1100\text{ cm}^{-1}$ . The band at  $500\text{-}600\text{ cm}^{-1}$  is assigned to the tetrahedral complex of Fe-O bond; however, a further TEM analysis was needed to determine the width of the coating.

Figure 4 shows the typical temperature curves (using the amplitude of 35 mT) obtained during the magnetic induction heating experiments of the particles with or without silica coating. The heating rate is proportional to the SAR value, and a direct relationship to the crystal size was observed. As evident in Figure 4, the smaller the particle, higher is the increase in temperature. In addition, we also found that that the increase in temperature was higher for particles coated with silica when compared to uncoated particles; however, this was independent of the particle size. Similar behavior was noticed when an amplitude of 63 mT was applied (Fig. 5). It is evident from Fig. 5 that after 2 min, the temperature of the 14 nm particles increases up to 35 °C and 27 °C with and without silica coating, respectively. This behavior could be explained considering the differences in their specific surface areas and heat capacities.

Table 1 presents the SAR values calculated using 35 and 63 mT are. Regarding the Eq. (1), a simple inspection of the variables involved shows that the main source of uncertainty in the measurements is the determination of the slope  $\Delta T/\Delta t$  (Huang *et al.*, 2012; Wang *et al.*, 2013). For this reason, the induction heating experiments were repeated three times to obtain the variance of the mean value. The SAR value obtained at 35 mT ( $\text{SAR}^1$ ) is smaller than that obtained at 63 mT ( $\text{SAR}^2$ ) due to its dependence with the magnetic field intensity. The temperature behavior shown in Figs 4 and 5 was, therefore, expected. The largest SAR value was observed in the smallest particles. This fact may be associated with polydispersity in sample sizes, indicating that the energy loss is due to the motion of magnetic domain walls and Neel relaxation mechanism that could decrease for large particles. Indeed, this phenomenon is consistent with the observations reported by Varadan *et al.* (2008). Additionally, an increase in the SAR value was observed to be approximately proportional to the square of the magnetic field amplitude.

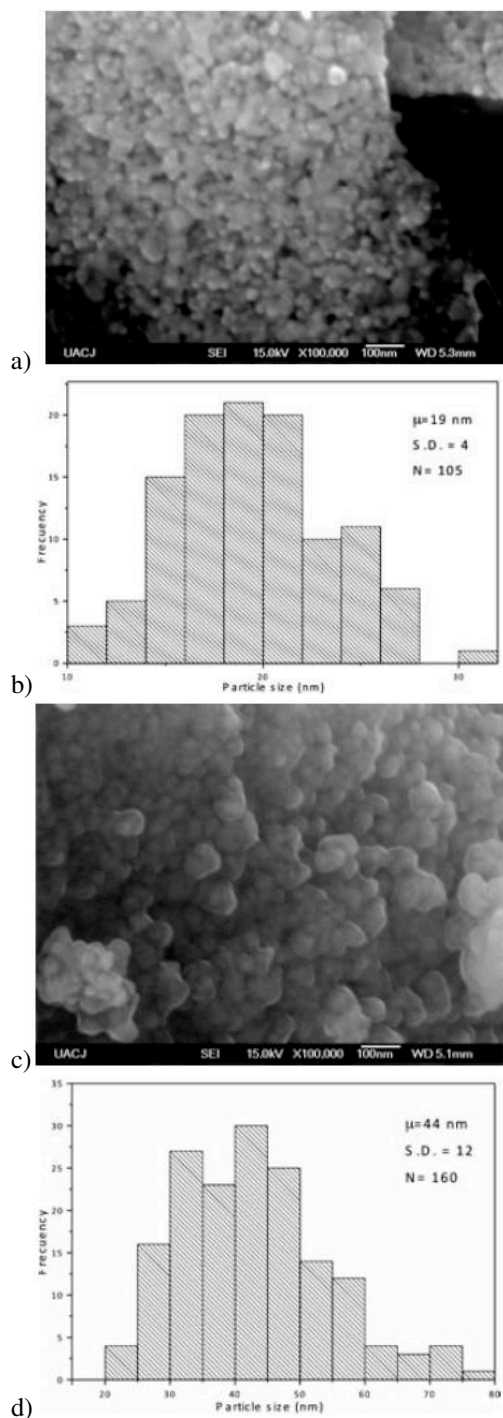


Fig. 2. SEM Images ((A) and (C)) and the particle size distribution ((B) and (D)) of CoFe<sub>2</sub>O<sub>4</sub> obtained at 500 and 700 °C respectively.

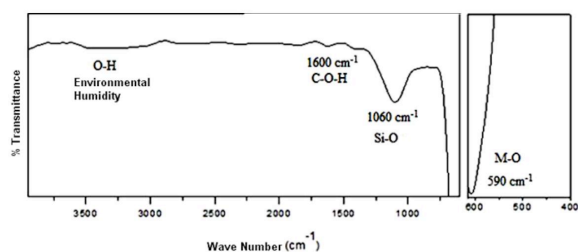


Fig. 3. FTIR spectra of CoFe<sub>2</sub>O<sub>4</sub>SiO<sub>2</sub>.

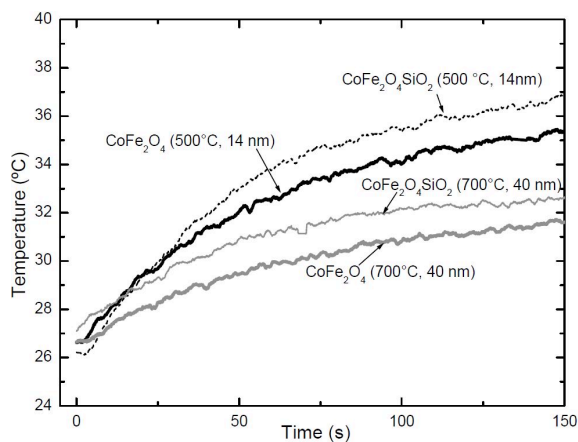


Fig. 4. Typical T vs. t curve of CoFe<sub>2</sub>O<sub>4</sub> and CoFe<sub>2</sub>O<sub>4</sub>SiO<sub>2</sub>, with different crystal size using an amplitude of 35 mT.

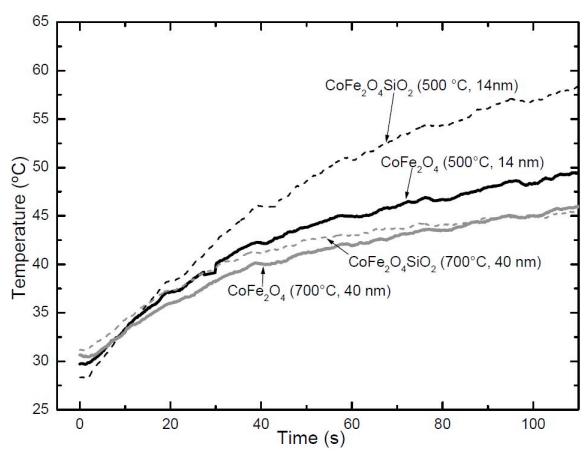
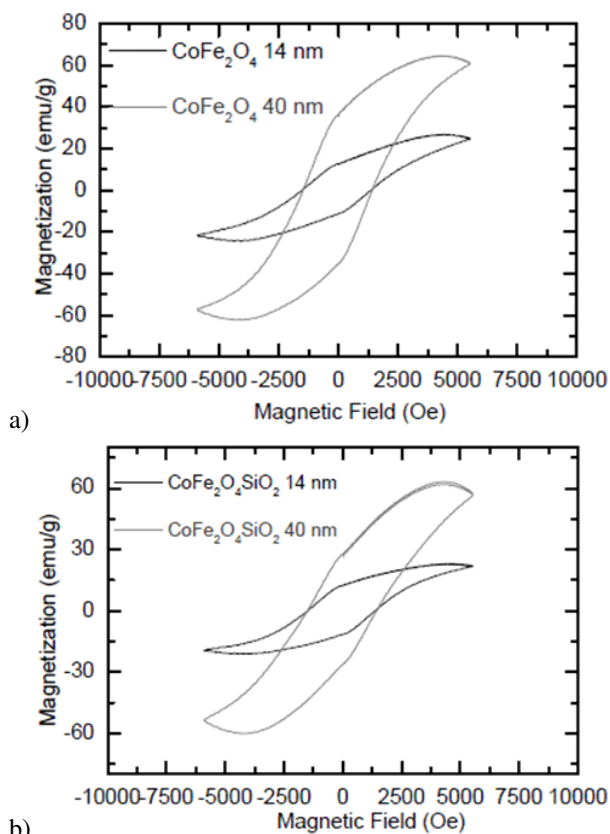
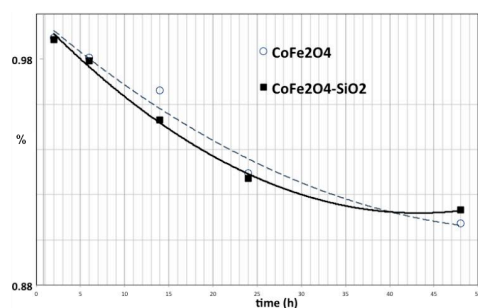


Fig. 5. Typical T vs. t curve of CoFe<sub>2</sub>O<sub>4</sub> and CoFe<sub>2</sub>O<sub>4</sub>SiO<sub>2</sub>, with different crystal size, using an amplitude of 63 mT.

Table 1. SAR Value Obtained Through Temperature vs Time Curve

Material	Core size (nm)	1/m (1)	$\Delta T/\Delta t^1$ ( $\times 10^{-1}$ (K/s))	$\Delta T/\Delta t^2$ ( $\times 10^{-1}$ (K/s))	$C_{NP}$ (J/gK)	$C_{eff}$ (J/gK)	SAR <sup>1</sup> (W/g)	SAR <sup>2</sup> (W/g)
CoFe <sub>2</sub> O <sub>4</sub>	14	12.0	1.40 ± 0.10	4.2 ± 0.5	0.28	3.87	6.50 ± 0.5	19.50 ± 2.3
CoFe <sub>2</sub> O <sub>4</sub> · SiO <sub>2</sub>	14	10.9	1.80 ± 0.15	5.5 ± 0.5	0.41	3.68	7.22 ± 0.6	22.06 ± 2.1
CoFe <sub>2</sub> O <sub>4</sub>	40	14.0	0.86 ± 0.04	3.2 ± 0.4	0.21	3.86	4.65 ± 0.2	17.29 ± 2.2
CoFe <sub>2</sub> O <sub>4</sub> · SiO <sub>2</sub>	40	13.7	0.84 ± 0.04	3.5 ± 0.5	0.25	3.80	4.37 ± 0.2	18.22 ± 2.1

Fig. 6. Hysteresis loops of CoFe<sub>2</sub>O<sub>4</sub> (A) and CoFe<sub>2</sub>O<sub>4</sub>SiO<sub>2</sub> (B) of different crystal size.Fig. 7. Degradation rate of CoFe<sub>2</sub>O<sub>4</sub> and CoFe<sub>2</sub>O<sub>4</sub>SiO<sub>2</sub> (square).

This is consistent with the equation of power dissipation per unit volume ( $P$ ) of the Rosensweig model Eq. (3) (Rosenweig, 2002).

$$P = \mu_0 \pi \chi'' f H_0^2 \quad (3)$$

Where  $\mu_0$  is the magnetic permeability of free space, and  $\chi''$  is the out-of phase component of the total magnetic susceptibility of the samples.

With both magnetic field amplitudes, the SAR<sup>1</sup> and SAR<sup>2</sup> values (columns 8 and 9) were found to be decreased when the particle size increased, as also observed by Veverka *et al.* (2007).

The hysteresis loops were obtained at room temperature using a VSM Lakeshore 4500 instrument, in a range of  $\pm 6000$  Oe to obtain the parameters of the magnetization. The particles exhibited a ferromagnetic behavior (Figs. 6A and B) and the remanence, saturation, and coercivity increased as function of the particles size. This is in agreement with Hrushikesh *et al.* (2009) and Veverka *et al.* (2007). A slight decrease in these parameters was observed after the silica coating probably due to the presence of diamagnetic material (SiO<sub>2</sub>). The decrease in SAR values with increasing particle size has also been observed by Veverka *et al.* (2007).

Figure 7 shows the degradation rate of the cobalt nanoparticles in a simulated body fluid with or without silica-coating. In both cases, they showed the similar trend, with the coated particles showing increase in the degradation rate. However, after 48 h, only less than 0.1% of material was lost. This small degradation implies that the nanoparticles can be used in a multifunctional system where first they can be used for drug delivery (duration of 45 h) and subsequently, be used to target malignant cells through the hyperthermia process.

## Conclusions

Our results showed that the specific absorption rate (SAR) of the cobalt ferrite depends on the particle size. Additionally, we also found that the use of silica coating onto the cobalt ferrite nanoparticles did not change the SAR significantly, for both particle sizes. This behavior is partially in agreement with Gonzalez-Fernandez *et al.* (2009) who reported insignificant differences in the specific power absorption (SPA) for the minor size particles of magnetite. Nevertheless, in order to find out the frequency of the magnetic field which optimizes the power absorption, following the theory of Rosensweig (2002), a further analysis of the SAR considering each hydrodynamic volume of particle is needed.

In addition, we also found a small degradation rate of the nanoparticles even after 48 h; however, the rate was comparatively faster in presence of the silica coating. This suggests that the cobalt ferrite nanoparticles might be suitable for multifunctional system with therapeutics purposes.

## Nomenclature

SAR	specific absorption rate (W/g)
$C_{eff}$	specific heat (J/(g*K))
$P$	power loss (W)
$f$	frequency of the AC magnetic field (Hz)
$H$	magnetic Field (T)
$T$	temperature (K)
<i>Greek symbols</i>	
$\mu_0$	magnetic Permeability of the free space (N/A <sup>2</sup> )
$\chi''$	complex magnetic susceptibility (cm <sup>3</sup> /g)

## References

- Cano, M.E., Barrera, A., Estrada, J.C., Hernández, A., Córdova, T. (2011). An induction heater device for studies of magnetic hyperthermia and SAR measurements. *Review of Scientific Instruments* 82, 114904-11498.
- Cano, M.E., Mazón, E.E., Hernández, A. and Alanis, M.E.E. (2012) Mx. Patent. Sol. Mx/a/2012/003963.
- Cornell R.M. and Udo, S. (2003). *The iron oxides: Structure, properties, reactions, occurrences, and uses*, 2nd. ed., Wiley-VCH, Germany.
- Cullity, B.D. and Graham C.D. (2009). *Introduction to magnetic materials*. 2nd. ed., Wiley, Piscataway, N.J.
- Gaumet, M., Vargas, A., Gurny, R. and Delie, F. (2008). Nanoparticles for drug delivery: The need for precision in reporting particle size parameters. *European Journal of Pharmaceutics and Biopharmaceutics* 69, 1-9.
- González-Fernández, M.A., Torres, T.E., Andrés-Vergés, M., R. Costo, de la Presa, P., Serna, C.J., Morales, M.P., Marquina, C., Ibarra, M.R. and Goya G.F. (2009). Magnetic nanoparticles for power absorption: Optimizing size, shape and magnetic properties. *Journal of Solid State Chemistry* 182, 2779-2784
- Goya, G.F., Lima, E.J., Arelaro, A.D., Torres, T., Rechenberg, H.R., Rossi, L., Marquina, C., and Ibarra M.R. (2008). Magnetic Hyperthermia With Fe<sub>3</sub>O<sub>4</sub> Nanoparticles: The Influence of Particle Size on Energy Absorption. *Institute of Electrical and Electronics Engineers Transactions on Magnetism* 44, 4444 - 4447.
- Hrushikesh M. Joshi, Yen Po Lin, Mohammed Aslam, P. V. Prasad, Elise A. Schultz-Sikma, Edelman, R., Meade, T. and Dravid, V.P. (2009). Effects of shape and size of cobalt ferrite nanostructures on their MRI contrast and thermal activation. *Journal of Physical Chemistry* 113, 17761-17767.
- Huang, S., Wang, S-Y., Gupta, A., Borca-Tasciuc, D.A., and Salon, S.J. (2012.) On the measurement technique for specific absorption rate of nanoparticles in an alternating electromagnetic field. *Measurements Science and Technology* 23, 035701 6pp.
- Martel-Estrada, S.A, Olivas-Armendáriz, I., Martínez-Pérez, C.A. and Chacón-Nava, J.G. (2012). *In vitro* Bioactivity of Chitosan/Poly(dl-lactide) Composites. *Revista Mexicana de Ingeniería Química* 11, 505-512.
- Ming Ma, Ya Wu, Jie Zhou, Yongkang Sun, Yu Zhang, Ning Gu. (2004). Size Dependence of Specific Power Absorption of Fe<sub>3</sub>O<sub>4</sub> Particles in AC Magnetic Field. *Journal of Magnetism and Magnetic Materials* 268, 33-39.
- Neuberger, T., Schöpf, B., Hofmann, H., Hofmann, M. and von Rechenberg, B.

- (2005). Superparamagnetic nanoparticles for biomedical applications: Possibilities and limitations of a new drug delivery system. *Journal of Magnetism and Magnetic Materials* 293, 483-496.
- O'Neili M.J. (1966). Measurement of Specific Heat Functions by Differential Scanning Calorimetry. *Analytical Chemistry* 38, 1331-1335.
- Rosensweig, R.E. (2002). Heating magnetic fluid with alternating magnetic field. *Journal of Magnetism and Magnetic Materials* 252, 370-374.
- Ruizhi Xu, Yu Zhang, Ming Ma, Jingguang Xia, Jiwei Liu, Quanzhong Guo, and Ning Gu, (2007). Measurement of Specific Absorption Rate and Thermal Simulation for Arterial Embolization Hyperthermia in the Maghemite-Gelled Model. *Institute of Electrical and Electronics Engineers Transactions on Magnetism* 43, 1078-1085
- Kelm, U. and Alfaro, G. (2011). Synthesis of Zeolites Nap-gis, with Different Morphologies, From Two Diatomites. *Revista Mexicana de Ingeniería Química* 10, 117-123.
- Varadan, V.K., Chen L. and Xie, J. (2008). *Nanomedicine: design and applications of magnetic nanomaterials, nanosensors*, 1 st. ed. Wiley & Sons. Ltd., Chichester U.K.
- Veverka, M., Veverka, P., Kaman, O., Lancok, A., Zaveta, K., Pollert, E., Knížek, K., Bohacek, J., Benes, M., Kaspar, P., Duguet E., and Vasseur, S. (2007). Magnetic heating by cobalt ferrite nanoparticles. *Nanotechnology* 18, 345704-345711.
- Wang, S.Y., Huang, S., and Borca-Tasciuc, D.A. (2013). Potential sources of errors in measuring and evaluating the specific loss power of magnetic nanoparticles in an alternating magnetic field. *Institute of Electrical and Electronics Engineers Transactions on Magnetism* 49, 255 - 262.
- Yeong II Kim, Y., Don Kim, D., Choong Sub Lee. (2003). Synthesis and characterization of CoFe<sub>2</sub>O<sub>4</sub> magnetic nanoparticles prepared by temperature-controlled coprecipitation method. *Physica B* 337, 42 - 51.